THE JOURNAL OF BIOLOGICAL CHEMISTRY
Vol. 280, No. 21, Issue of May 27, pp. 20404–20412, 2005
Printed in U.S.A.

Encephalitozoon cuniculi mRNA Cap (Guanine N-7) Methyltransferase

METHYL ACCEPTOR SPECIFICITY, INHIBITION BY *S*-ADENOSYLMETHIONINE ANALOGS, AND STRUCTURE-GUIDED MUTATIONAL ANALYSIS*

Received for publication, January 28, 2005, and in revised form, February 17, 2005
Published, JBC Papers in Press, March 9, 2005, DOI 10.1074/jbc.M501073200

Stéphane Hausmann‡, Sushuang Zheng‡, Carme Fabrega‡, Stewart W. Schneller§, Christopher D. Lima‡, and Stewart Shuman‡¶

From the ‡Molecular Biology and Structural Biology Programs, Sloan-Kettering Institute, New York, New York 10021 and §Department of Chemistry and Biochemistry, Auburn University, Auburn, Alabama 36849

The *Encephalitozoon cuniculi* mRNA cap (guanine N-7) methyltransferase Ecm1 has been characterized structurally but not biochemically. Here we show that purified Ecm1 is a monomeric protein that catalyzes methyl transfer from *S*-adenosylmethionine (AdoMet) to GTP. The reaction is cofactor-independent and optimal at pH 7.5. Ecm1 also methylates GpppA, GDP, and dGTP but not ATP, CTP, UTP, ITP, or m^{7}GTP. The affinity of Ecm1 for the cap dinucleotide GpppA (K_m 0.1 mM) is higher than that for GTP (K_m 1 mM) or GDP (K_m 2.4 mM). Methylation of GTP by Ecm1 in the presence of 5 μM AdoMet is inhibited by the reaction product AdoHcy (IC_{50} 4 μM) and by substrate analogs sinefungin (IC_{50} 1.5 μM), aza-AdoMet (IC_{50} 100 μM), and carbocyclic aza-AdoMet (IC_{50} 35 μM). The crystal structure of an Ecm1·aza-AdoMet binary complex reveals that the inhibitor occupies the same site as AdoMet. Structure-function analysis of Ecm1 by alanine scanning and conservative substitutions identified functional groups necessary for methyltransferase activity *in vivo*. Amino acids Lys-54, Asp-70, Asp-78, and Asp-94, which comprise the AdoMet-binding site, and Phe-141, which contacts the cap guanosine, are essential for cap methyltransferase activity *in vitro*.

The 5′ cap of eukaryotic messenger RNA consists of 7-methyl guanosine linked via an inverted 5′–5′ triphosphate bridge to the initiating nucleoside of the transcript. The cap is formed by three enzymatic reactions: (i) the 5′-triphosphate end of the pre-mRNA is hydrolyzed to a diphosphate by RNA 5′-triphosphatase; (ii) the diphosphate RNA end is capped with GMP by RNA guanylyltransferase; and (iii) the GpppN cap is methylated by RNA (guanine N-7) methyltransferase. This pathway is conserved in all eukaryotic organisms and many eukaryotic viruses (1). The capping enzymes are considered attractive targets for antiviral, antifungal, and antiprotozoal drug discovery (2).

RNA guanine N-7 methyltransferase catalyzes transfer of a methyl group from *S*-adenosylmethionine (AdoMet)[1] to GpppRNA to form m^{7}GpppRNA and *S*-adenosylhomocysteine (AdoHcy). Vaccinia virus cap methyltransferase has been extensively characterized with respect to its substrate specificity (3, 4). The poxvirus methyltransferase is a heterodimeric protein composed of a catalytic subunit and a stimulatory subunit; the catalytic subunit contains the sites for substrate binding and catalysis but is only weakly active on its own (5–11). In contrast, cellular cap methyltransferases are monomeric enzymes that resemble the catalytic subunit of the poxvirus methyltransferase with respect to primary structure and the effects of mutations at certain essential residues that are proposed to comprise the active site (12–16). The *Saccharomyces cerevisiae* cap methyltransferase Abd1 has been extensively characterized genetically, but biochemical studies are not as far advanced (12–15). Cap methyltransferase orthologs have been identified in humans and other fungi (16–19), but these enzymes are also not well characterized biochemically.

Our recent studies have focused on the cap methyltransferase Ecm1 from the microsporidian parasite *Encephalitozoon cuniculi* (20, 21). Ecm1 is the smallest cap methyltransferase known (298-aa), and it contains all of the essential components for cap methyltransferase activity *in vivo*, as gauged by complementation in yeast (20). We have crystallized Ecm1 and determined its structure by x-ray diffraction (21). Ecm1 contains two ligand-binding pockets, one for the methyl donor AdoMet and one for the cap guanosine methyl acceptor and the 5′-triphosphate of the cap. Superposition of the structures of Ecm1·ligand complexes suggested a direct in-line mechanism of methyl transfer. No Ecm1 residues were observed in contact with the guanine N-7 nucleophile, the AdoMet methyl carbon, or the AdoHcy sulfur leaving group, implying that Ecm1 facilitates methyl transfer to cap guanine N-7 by optimizing proximity and geometry of the donor and acceptor. A similar catalytic strategy is used by glycine *N*-methyltransferase (22).

The crystal structures of Ecm1 provided clues to cap recognition and a potential scaffold for structure-based inhibitor design. The limitation to exploiting the structural information is that there has been no biochemical analysis of the cap methyltransferase activity imputed to Ecm1. Here we have shown that Ecm1 is a guanine-specific methyltransferase, determined its methyl acceptor preferences, and interpreted the findings in light of the enzyme structure. We have analyzed inhibition by

* This work was supported by National Institutes of Health Grants GM52470 (to S. S.), GM61906 (to C. D. L.), and AI56540 (to S. W. S.). The costs of publication of this article were defrayed in part by the payment of page charges. This article must therefore be hereby marked "*advertisement*" in accordance with 18 U.S.C. Section 1734 solely to indicate this fact.

The atomic coordinates and structure factors (code 1Z3C) have been deposited in the Protein Data Bank, Research Collaboratory for Structural Bioinformatics, Rutgers University, New Brunswick, NJ (http://www.rcsb.org/).

¶ An American Cancer Society research professor. To whom correspondence should be addressed. E-mail: s-shuman@ski.mskcc.org.

[1] The abbreviations used are: AdoMet, *S*-adenosylmethionine; AdoHcy, *S*-adenosylhomocysteine; m^{7}GTP, 7-methyl-GTP; DTT, dithiothreitol; 5-FOA, 5-fluoroorotic acid; XTP, xanthosine 5′-triphosphate; TLC, thin layer chromatography; VDW, van der Waals.

the product AdoHcy and several substrate analogs and presented the structure of the analog aza-AdoMet in complex with Ecm1. We have conducted a structure-guided functional analysis of the active site of Ecm1 by gauging effects of mutations on methyltransferase activity *in vivo* and *in vitro*.

EXPERIMENTAL PROCEDURES

Materials—[^{3}H-CH$_3$]AdoMet was purchased from PerkinElmer Life Sciences. GTP, GDP, m^{7}GTP, ATP, UTP, CTP, ITP, AdoMet, AdoHcy, and sinefungin were purchased from Sigma. GpppA was purchased from New England Biolabs. 3′-OMeGTP was from Amersham Biosciences. aza-AdoMet and carbocyclic aza-AdoMet were synthesized as described (23).

Recombinant Ecm1—An NdeI/BamHI fragment encoding the wild-type Ecm1 polypeptide was inserted into the bacterial expression vector pET16b. The pET-Ecm1 plasmid was transformed into *Escherichia coli* BL21(DE3). A 500-ml culture of *E. coli* BL21(DE3)/pET-Ecm1 was grown at 37 °C in Luria-Bertani medium containing 0.1 mg/ml ampicillin until the A_{600} reached ~0.6. The culture was placed on ice for 30 min and then adjusted to 0.2 mM isopropyl 1-thio-β-D-galactopyranoside and 2% (v/v) ethanol. After further incubation for 17 h at 18 °C with constant shaking, the cells were harvested by centrifugation. The cell pellet was stored at −80 °C. All subsequent procedures were performed at 4 °C. Thawed bacteria were resuspended in 30 ml of buffer A (50 mM Tris-HCl, pH 7.5, 200 mM NaCl, 10% glycerol). Phenylmethylsulfonyl fluoride and lysozyme were added to final concentrations of 300 μM and 100 μg/ml, respectively. After incubation on ice for 30 min, Triton X-100 was added to a final concentration of 0.1%, and the lysate was sonicated to reduce viscosity. Insoluble material was removed by centrifugation for 45 min at 18,000 rpm in a Sorvall SS34 rotor. The soluble extract was mixed for 30 min with 2 ml of Ni^{+2}-nitrilotriacetic acid-agarose (Qiagen) that had been equilibrated with buffer A containing 0.1% Triton X-100 and 10 mM imidazole. The slurry was poured into a column, and the resin was washed with 10 ml of 10 and 20 mM imidazole in buffer A. Adsorbed protein was then serially step-eluted with 3-ml aliquots of 50, 100, 250, and 500 mM imidazole in buffer A. The polypeptide compositions of the column fractions were monitored by SDS-PAGE. The 250 mM imidazole eluate fraction containing His$_{10}$-Ecm1 (10 mg of protein) was dialyzed against 50 mM Tris-HCl, pH 7.5, 200 mM NaCl, 2 mM DTT, 1 mM EDTA, 0.01% Triton X-100, and 10% glycerol and then stored at −80 °C. Protein concentration was determined using the Bio-Rad dye reagent with bovine serum albumin as the standard.

An aliquot (45 μg) of the nickel-agarose preparation of His$_{10}$-Ecm1 was mixed with bovine serum albumin (40 μg) and cytochrome *c* (40 μg) in 0.2 ml of buffer G (50 mM Tris-HCl, pH 8.0, 100 mM NaCl, 1 mM EDTA, 2 mM DTT, 0.05% Triton X-100). The mixtures were layered onto a 4.8-ml 15–30% glycerol gradient containing buffer G. The gradient was centrifuged in a Beckman SW50 rotor at 50,000 rpm for 17 h at 4 °C. Fractions (0.2 ml) were collected from the bottom of the tube.

Methyltransferase Assay—Reaction mixtures (20-μl) containing 50 mM Tris-HCl, pH 7.5, 5 mM DTT, 5 mM GTP, [^{3}H-CH$_3$]AdoMet, and Ecm1, as specified, were incubated for 60 min at 37 °C. Aliquots (16 μl) were spotted onto DEAE-cellulose filters (25-mm, Whatman DE81), which were washed three times batch-wise with 20 mM ammonium bicarbonate. The filters were dried, and the radioactivity adsorbed to the filter was quantified by liquid scintillation counting.

Mutational Effects on Ecm1 Function in Vivo—Missense mutations were introduced into the *ECM1* gene by the PCR-based two-stage overlap extension method. The mutated genes were inserted into the yeast *CEN TRP1* plasmid p358-ECM1, where expression of *ECM1* is under the control of the natural *ABD1* promoter (21). The inserts were sequenced completely to exclude the acquisition of unwanted mutations during amplification and cloning. The *in vivo* activity of the mutated *ABD1* alleles was tested by plasmid shuffle (20, 21). Yeast strain YBS40 (*Mat***a** *leu2 ade2 trp1 his3 ura3 can1 abd1*::*hisG* p360-ABD1[*CEN URA3 ABD1*]) was transformed with *CEN TRP1* plasmids containing the wild-type and mutant alleles of *ECM1*. Trp$^+$ isolates were selected and then streaked on agar plates containing 0.75 mg/ml 5-fluoroorotic acid (5-FOA). Growth was scored after 7 days of incubation at 25, 30, and 37 °C. Lethal mutants were those that failed to form colonies on 5-FOA at any temperature. Individual colonies of the viable *ECM1* mutants were picked from the 5-FOA plate and transferred to YPD (yeast extract/peptone/dextrose) agar medium. Two isolates of each mutant were tested for growth on YPD agar at 25, 30, and 37 °C. Growth was assessed as follows: +++ indicates colony size indistinguishable from strains bearing wild-type *ECM1*; ++ denotes slightly reduced colony size; + indicates that only pinpoint colonies were formed; and − indicates no growth.

Mutational Effects on Ecm1 Function in Vivo—NdeI/BamHI fragments encoding Ecm1-Ala mutants K54A, D70A, D78A, D94A, and Y141A were excised from the respective p358-ECM1 plasmids and inserted into pET16b. The pET16-Ecm1-Ala plasmids were introduced into *E. coli* BL21(DE3). The recombinant Ecm1-Ala proteins were produced and purified from soluble bacterial lysates as described above for wild-type Ecm1.

Crystal Structure of Ecm1 Bound to aza-AdoMet—Ecm1 was produced for crystallographic analysis as reported previously (21). Ecm1 was incubated with 1 mM aza-AdoMet for 30 min prior to crystallization by vapor diffusion against a well solution containing 1.2 M sodium/potassium tartrate, 50 mM bis(2-hydroxyethyl)amino-tris(hydroxymethyl)methane (pH 6.0 or 6.25), and 20 mM DTT. Crystals were cryoprotected with well solution containing 18% glycerol. Crystals diffracted x-rays to 2.2 Å ($P3_121$, $a = b = 63.25$ Å, $c = 111.84$ Å, $\alpha = \beta = 90°$, $\gamma = 120°$). Data were collected at National Synchrotron Light Source beamline X4A (Brookhaven, NY) using an ADSC quantum-4 charge-couple device detector. Data were reduced with DENZO, SCALEPACK (24), and CCP4 (25) software. The Ecm1·aza-AdoMet complex was isomorphous to the previously determined crystal structures of Ecm1 (21). Electron density maps were interpreted using O software (26), and models were refined using crystallography NMR software (27) to an R_{cryst} of 0.22 and R_{free} of 0.27. The model has excellent geometry with no Ramachandran outliers. The coordinates have been deposited in the Protein Data Bank (accession code 1Z3C).

RESULTS

Methyltransferase Activity of Recombinant Ecm1—Ecm1 was produced in *E. coli* as a His$_{10}$-Ecm1 fusion and purified from a soluble extract by nickel-affinity chromatography. The His$_{10}$-Ecm1 protein was adsorbed to the resin and recovered in the 100–500 mM imidazole eluate fractions (Fig. 1*A*). Further characterization of Ecm1 was performed using the 250 mM imidazole fraction. The quaternary structure was examined by zonal velocity sedimentation in a 15–30% glycerol gradient. Marker proteins catalase (native size 248 kDa), bovine serum albumin (66 kDa) and cytochrome *c* (12 kDa) were included as internal standards in the gradient. After centrifugation, the polypeptide compositions of the odd numbered gradient fractions were analyzed by SDS-PAGE. His$_{10}$-Ecm1 (calculated to be a 40-kDa polypeptide) sedimented as a discrete peak (fractions 19–21) between bovine serum albumin and cytochrome *c* (Fig. 1*B*).

The methyltransferase activity was demonstrated by incubating the gradient fractions with 5.4 μM [^{3}H-CH$_3$]AdoMet and 5 mM GTP for 60 min at 37 °C, which resulted in label transfer from AdoMet to the GTP to form an anionic methylated nucleotide product that was adsorbed to a DEAE filter and thereby separated from the cationic AdoMet substrate (28). The extent of ^{3}H-methyl transfer paralleled the abundance of the Ecm1 polypeptide and peaked at fractions 19–20 (Fig. 1*B*). These results imply a monomeric structure for Ecm1 in solution, which is consistent with the finding that Ecm1 crystallized as a monomer (21). Methyl transfer by Ecm1 was optimal at pH 7.5 in Tris buffer and declined sharply at pH <6.0 (Fig. 1*C*).

Methyl Acceptor Specificity—Various nucleotides were tested as methyl acceptors at 5 mM concentration (Fig. 2). Ecm1 methylated GTP and dGTP but not ATP, CTP, or UTP (Fig. 2*A*). Thus, Ecm1 is a guanine-specific methyltransferase that does not discriminate between ribose and deoxyribose nucleoside sugars. The putative reaction product, m^{7}GTP, was not methylated by Ecm1, as expected (Fig. 2*B*). Failure to methylate ITP indicates that the exocyclic 2′-amine of guanine is essential for substrate recognition. Failure to methylate XTP shows that Ecm1 discriminates between an amine and a carbonyl at position 2 of the purine ring. Methyl transfer to GDP was 40% as effective as that to GTP. 3′-OMeGTP was about one-third as effective as GTP and dideoxy-GTP was one-fourth as effective as GTP (Fig. 2).

The dependence of the extent of methyl transfer on GTP concentration is shown in Fig. 3, *left panel*. From a double-reciprocal plot of the data, we calculated a K_m of 1 mM GTP. The

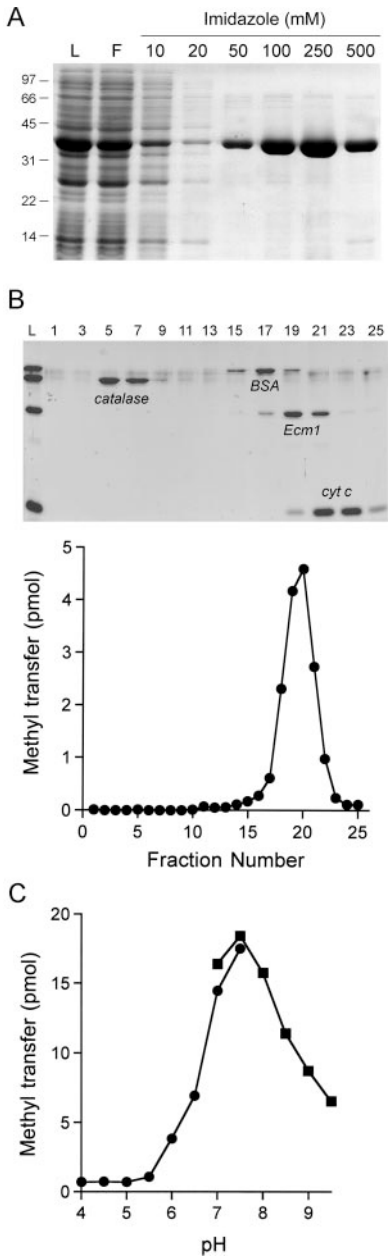

FIG. 1. **Methyltransferase activity of recombinant Ecm1.** *A*, Ecm1 purification. Aliquots (10 μl) of the soluble bacterial lysate (*L*), the nickel-agarose flow-through (*F*), and the 10, 20, 50, 100, 250, and 500 mM imidazole eluate fractions were analyzed by SDS-PAGE. The polypeptides were visualized by staining with Coomassie Blue dye. The positions and sizes (kDa) of marker polypeptides are indicated on the *left*. *B*, velocity sedimentation was performed as described under "Experimental Procedures." Aliquots (16 μl) of the input protein mixture (*L*) and the odd-numbered glycerol gradient fractions were analyzed by SDS-PAGE. The Coomassie Blue-stained gel is shown in the *upper panel*. The identities of the polypeptides are indicated. The methyltransferase activity profile is shown in the *lower panel*. Reaction mixtures (20 μl) contained 5 mM GTP, 5.4 μM [^{3}H-CH$_3$]AdoMet, and 4 μl of the indicated glycerol gradient fractions. *BSA*, bovine serum albumin; *cyt c*, cytochrome *c*. *C*, pH dependence. Reaction mixtures (20 μl) containing 50 mM Tris buffer (either Tris acetate (●), pH 4.0, 4.5, 5.0, 5.5, 6.0, 6.5, 7.0, or 7.5 or Tris-HCl (■), pH 7.0, 7.5, 8.0, 8.5, 9.0, or 9.5), 5 mM DTT, 5 mM GTP, 5.4 μM [^{3}H-CH$_3$]AdoMet and 2 μg of Ecm1 were incubated for 60 min at 37 °C. The formation of labeled product that adsorbed to DE81 filters is plotted as a function of pH.

cap dinucleotide GpppA was a more effective methyl acceptor than GTP at submillimolar concentrations; from the dependence of methyl transfer on GpppA concentration (Fig. 3, *right panel*), we calculated a K_m of 0.1 mM GpppA. The K_m for GDP

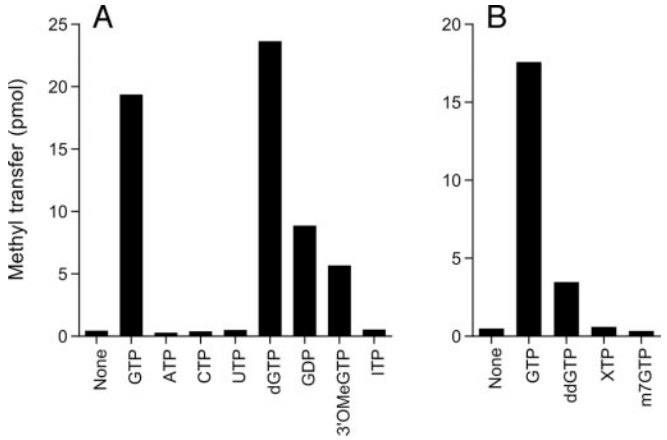

FIG. 2. **Methyl acceptor specificity of Ecm1.** Reaction mixtures (20 μl) containing 50 mM Tris-HCl, pH 7.5, 5 mM DTT, 5.4 μM [^{3}H-CH$_3$]AdoMet, 5 mM of the specified nucleotide (or no nucleotide where indicated), and 2 μg of Ecm1 were incubated for 60 min at 37 °C. The extents of methyl transfer to yield DE81-absorbable material are shown.

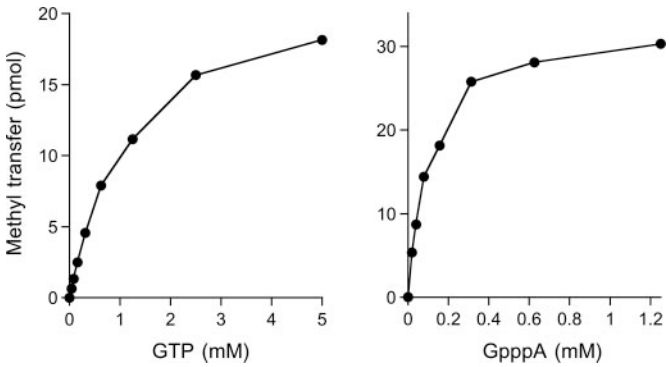

FIG. 3. **Methyl acceptor dependence.** Reaction mixtures (20 μl) containing 50 mM Tris-HCl, pH 7.5, 5 mM DTT, 5.4 μM [^{3}H-CH$_3$]AdoMet, 2 μg of Ecm1, and either GTP (*left panel*) or GpppA (*right panel*), as specified, were incubated for 60 min at 37 °C. The extents of methyl transfer to yield DE81-absorbable material are plotted as a function of methyl acceptor concentration.

was 2.4 mM (data not shown). Thus the affinity of Ecm1 for the guanine nucleotide methyl acceptor is enhanced by 2-fold by the γ phosphate of GTP and 10-fold by the 5′-nucleoside of the RNA component of GpppA, a more "physiological" mimic of the presumed GpppRNA substrate.

Inhibition by the Product AdoHcy and Substrate Analogs Sinefungin and aza-AdoMet—The chemical structures of the substrate AdoMet and the product AdoHcy are shown in Fig. 4. The extent of GTP methylation by Ecm1 increased with [^{3}H-CH$_3$]AdoMet concentration; from a double-reciprocal plot of the data (not shown), we calculated a K_m of 25 μM AdoMet. Activity in the presence of 5.4 μM [^{3}H-CH$_3$]AdoMet was inhibited in a concentration-dependent fashion by AdoHcy; the apparent IC$_{50}$ for AdoHcy was 4 μM (Fig. 5). We surmise that Ecm1 has similar affinities for the substrate AdoMet and the product AdoHcy.

Sinefungin is an analog of AdoMet that has been shown to have antifungal, antiprotozoal, and antiviral activities (29, 30). Sinefungin differs from AdoMet in that the S-CH$_3$ sulfonium moiety is replaced by a C-NH$_2$ secondary amine (Fig. 4). Although sinefungin is an inhibitor of a variety of AdoMet-dependent methyltransferases, it has been suggested that its antiviral properties reflect selective inhibition of virus-encoded cap methyltransferases (30). To our knowledge, the effects of sinefungin on a cellular cap-methylating enzyme have not been reported. Here we found that Ecm1 was inhibited by sinefungin in a concentration-dependent manner, with an apparent IC$_{50}$ of 1.5 μM (Fig. 5*B*). We infer than

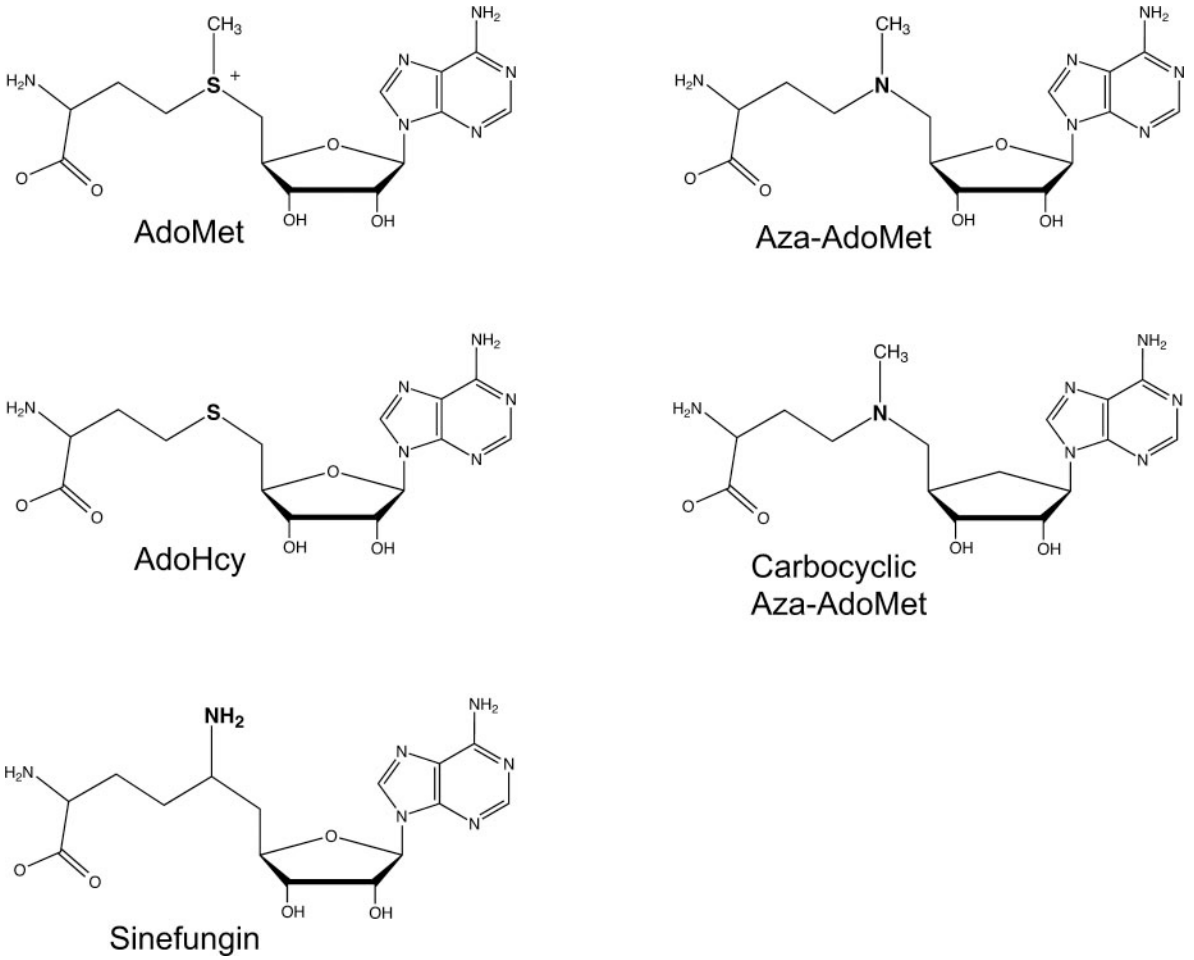

FIG. 4. **Chemical structures of AdoMet, AdoHcy, and analogs sinefungin, aza-AdoMet, and carbocyclic aza-AdoMet.**

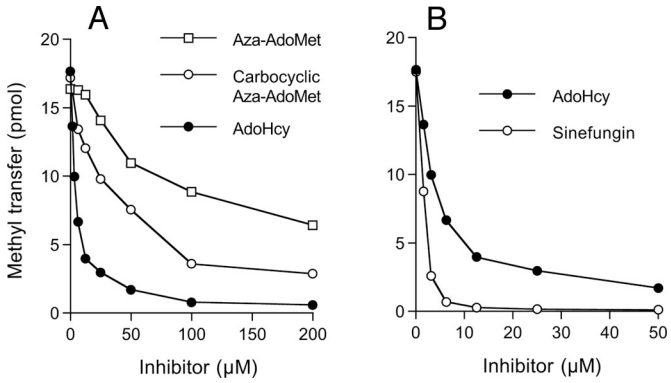

FIG. 5. **Inhibition of methyltransferase activity.** Reaction mixtures (20 μl) containing 50 mM Tris-HCl, pH 7.5, 5 mM DTT, 5 mM GTP, 5.4 μM [^{3}H-CH$_3$]AdoMet, 2 μg of Ecm1, and either AdoHcy, aza-AdoMet, carbocyclic aza-AdoMet, or sinefungin, as specified, were incubated for 60 min at 37 °C. The extents of methyl transfer to yield DE81-absorbable material are plotted as a function of AdoHcy, aza-AdoMet, carbocyclic aza-AdoMet, or sinefungin concentration.

Ecm1 has a 2- to 3-fold higher affinity for sinefungin than it does for AdoMet or AdoHcy.

aza-AdoMet is a substrate analog in which the sulfur is replaced by nitrogen (Fig. 4) (31, 32). The carbocyclic derivative of aza-AdoMet has a methylene group in lieu of the ribose O-4 atom (Fig. 4) (23). aza-AdoMet and carbocyclic aza-AdoMet were relatively weak inhibitors of Ecm1, with IC_{50} values of 100 and 35 μM, respectively (Fig. 5*A*).

Product Analysis—The products of the reaction of Ecm1 with 5 mM GTP and 5.4 μM [^{3}H-CH$_3$]AdoMet were analyzed by polyethyleneimine-cellulose thin layer chromatography (TLC) in parallel with a control reaction from which Ecm1 was omitted (Fig. 6). The chromatogram was developed with 0.2 M ammonium sulfate, which allowed resolution of GTP and m^{7}GTP from AdoMet. The positions of unlabeled nucleotide standards were identified by UV shadowing. The distribution of ^{3}H radioactivity was gauged by cutting the chromatogram into 1-cm strips and quantifying each strip by liquid scintillation counting. Most of the radioactivity in the no-enzyme control comigrated with AdoMet, and there was no radioactivity associated with the guanine nucleotides (Fig. 6, *bottom panel*). In the presence of Ecm1, the [^{3}H-CH$_3$]AdoMet was depleted and the label transferred to a single product comigrating with the m^{7}GTP standard. About 70% of the input label was converted to m^{7}GTP product in this experiment.

The TLC assay was used to gauge the specific activity and kinetics of methyl transfer in reactions containing 50 μM AdoMet, 5 mM GTP, and varying amounts of Ecm1. The AdoMet- and m^{7}GTP-containing portions of the TLC plate were excised, and the distribution of radiolabel was quantified by liquid scintillation counting. The specific activity calculated from the slope of the titration curve in Fig. 7*A* was ~2.5 pmol of methyl transfer/pmol of Ecm1. A kinetic analysis showed that methylated GTP product accumulated steadily during a 120-min incubation (Fig. 7*B*), implying that the enzyme was not inactivated during the incubation and that Ecm1 did not catalyze a rapid burst of methylation, with subsequent rounds limited by slow product release. The initial rate was proportional to Ecm1 concentration. The extent of methyl transfer by the highest level of Ecm1 at 120 min corresponded to 40% of the input [^{3}H-CH$_3$]AdoMet substrate.

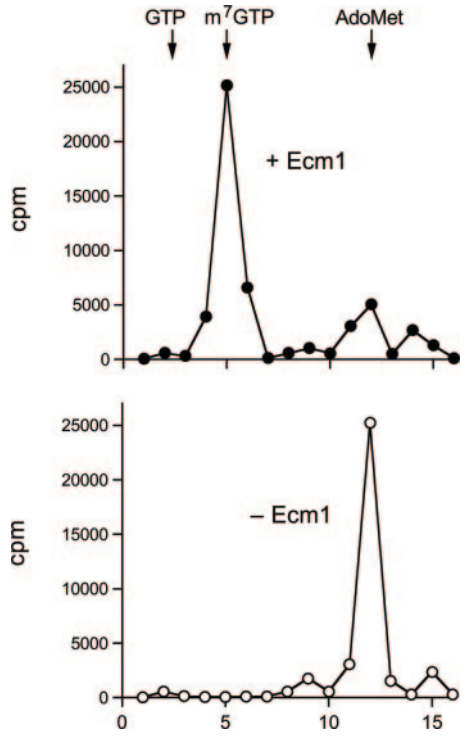

FIG. 6. **TLC analysis of the methylation reaction product.** Reaction mixtures (20 μl) containing 50 mM Tris-HCl, pH 7.5, 5 mM DTT, 5 mM GTP, 5.4 μM [^{3}H-CH$_3$]AdoMet, and either 3 μg of Ecm1 (*top panel*) or no enzyme (*bottom panel*) were incubated for 60 min at 37 °C. Aliquots (5 μl) were spotted onto a polyethyleneimine cellulose TLC plate, which was developed with 0.2 M $(NH_4)_2SO_4$. Marker nucleotides were located by UV illumination. The lanes were cut into 1-cm strips, and radioactivity was quantified by liquid scintillation counting. *cpm*, counts/min.

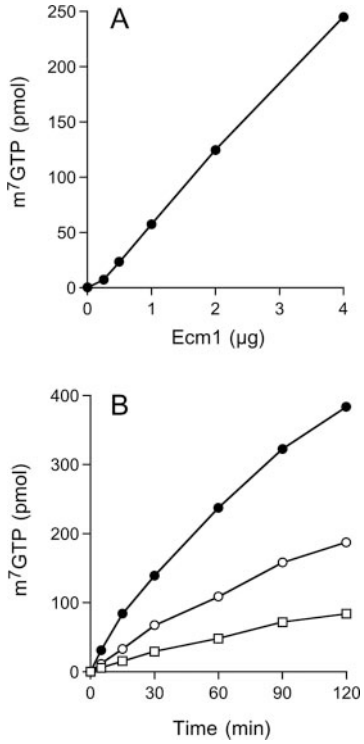

FIG. 7. **Enzyme dependence and kinetics of m^{7}GTP synthesis.** *A*, Ecm1 titration. Reaction mixtures (20 μl) containing 50 mM Tris-HCl (pH 7.5), 5 mM DTT, 5 mM GTP, 50 μM [^{3}H-CH$_3$]AdoMet and Ecm1 as specified were incubated for 60 min at 37 °C. Aliquots (5 μl) were spotted on polyethyleneimine cellulose TLC plates, which were developed with 0.2 M $(NH_4)_2SO_4$. The extent of [^{3}H-CH$_3$]m^{7}GTP formation is plotted as a function of input Ecm1. *B*, kinetics. Reaction mixtures (60 μl) containing 50 mM Tris-HCl (pH 7.5), 5 mM DTT, 5 mM GTP, 50 μM [^{3}H-CH$_3$]AdoMet and either 12 μg (●), 6 μg (○) or 3 μg (□) of Ecm1 were incubated at 37 °C. Aliquots (5 μl) were withdrawn at the times indicated and spotted on polyethyleneimine cellulose TLC plates, which were developed with 0.2 M $(NH_4)_2SO_4$. The extent of [^{3}H-CH$_3$]m^{7}GTP formation is plotted as a function of time.

Structure of Ecm1 in Complex with aza-AdoMet—A structure was determined for Ecm1 in complex with the weak inhibitor aza-AdoMet (Table I and Fig. 8*A*). The 2.2-Å simulated annealing omit density map of the ligand is shown in Fig. 8*B* contoured at 1.0σ. aza-AdoMet is bound in a manner virtually identical to that of AdoMet reported previously (21). The adenine base of aza-AdoMet is sandwiched between Tyr-124 and Ile-95 through van der Waals (VDW) contacts. Direct hydrogen bonding interactions are observed between adenine N-6 and Asp-122 O-δ, whereas a more distant hydrogen bond is observed between adenine N-1 and Ser-123 O-γ. The ribose O-2′ and O-3′ atoms are coordinated via bidentate hydrogen bonding to the Asp-94 carboxylate, whereas the ribose O-4′ is in VDW contact with Ser-142. The carboxylate oxygen and amino nitrogen atoms of aza-AdoMet make hydrogen bonds with the Lys-54 N-ζ and the backbone carbonyl oxygen atoms of Gln-140 and Gly-72, respectively. Also, both Asp-70 and Asp-78 O-δ atoms make water-mediated contacts to the amino nitrogen and carbonyl oxygen atoms of aza-AdoMet. Structural comparison of the aza-AdoMet, AdoMet, and AdoHcy complexes with Ecm1 revealed no substantive differences in protein or ligand conformations within coordinate error. Thus, aza-AdoMet is a competitive inhibitor for the methyl donor site on Ecm1.

Mutational Analysis of Ecm1—The wild-type *ECM1* gene on a centromeric plasmid under the control of the *ABD1* promoter is capable of complementing growth of an *S. cerevisiae abd1*Δ strain (21). In a previous study, we tested the effects of several single-alanine and double-alanine substitutions on Ecm1 function in yeast and thereby identified mutations in components of the GTP and AdoMet-binding pockets that were either lethal or elicited a temperature-sensitive growth defect (21). Here we extended the alanine scan to new residues and determined structure/activity relationships by testing the effects of conservative substitutions. The choice of residues to mutate was guided by the available crystal structures of Ecm1·ligand complexes. Whereas most of the residues mutated were either in direct contact with (or near) the GTP methyl acceptor or the AdoMet donor, we also chose to target several basic side chains on the surface of Ecm1 (Arg-59, Arg-84, and Lys-267) that we thought might contribute to a hypothetical RNA docking site distal to the triphosphate bridge of GTP (Fig. 8*C*). All mutant *ECM1* alleles were placed under control of the *ABD1* promoter on a centromeric plasmid and assayed by plasmid shuffle for *abd1*Δ complementation. Lethal mutations were those that failed to support the appearance of 5-FOA-resistant colonies at 25, 30, or 37 °C (scored as − at all temperatures). The viable FOA-resistant *ECM1* strains were tested for growth on rich medium (YPD agar) at 25, 30, and 37 °C. Growth was scored as follows: +++ indicates colony size indistinguishable from strains bearing wild-type *ECM1*; ++ denotes reduced colony size; + indicates that only pinpoint colonies were formed; − indicates no growth.

Residues Lys-54, Asp-70, Asp-78, and Asp-94 that comprise the AdoMet-binding pocket are all essential for Ecm1 function in yeast, *i.e.* alanine substitutions at each of these positions were lethal. Lys-54 coordinates the carboxylate of AdoMet (Fig. 8*A*). This essential contact is strictly dependent on lysine, insofar as the conservative K54R and K54Q mutations failed to restore growth (Table II). Asp-70 makes a pair of water-mediated interactions with the amine of AdoMet, and Asp-94 makes a pair of direct contacts with the AdoMet ribose 2′-OH and

TABLE I
Crystallographic data and refinement statistics

	Ecm1-AzoAdoMet
PDB ID	1Z3C
Source	National Synchrotron Light Source X4A
Wavelength (Å)	0.9790
Resolution limits (Å)	20–2.2
Space group	$P3_121$
Unit cell (Å) *a, b, c, α, β, γ*	63.25, 63.25, 111.84, 90, 90, 120
Number of observations	58,215
Number of reflections	13,451
Completeness (%)	97.9 (95.7)[d]
Mean $I/\sigma I$	10.9 (4.9)
R-merge on I[a]	8.4 (33.3)
Cut-off criteria $I/\sigma I$	−0.5
Refinement Statistics	
Resolution limits (Å)	20–2.2
Number of reflections	13288
Completeness (%)	97.2 (93.6)
Cutoff criteria $I/\sigma I$	0
Protein/ligand/water atoms	2062/27/132
R_{cryst}[b]	0.222 (0.424)
R_{free} (5% of data)	0.270 (0.454)
Bonds (Å)[c]	0.006
Angles (°)[c]	1.1
B-factor (mc/sc in Å^2)[c]	1.45/2.12

[a] $R_{merge} = \Sigma\Sigma_{hkl}\,\Sigma_i|I(hkl)i - \langle I(hkl)\rangle|/\Sigma_{hkl}\Sigma_i\langle I(hkl)_i\rangle$.
[b] $R_{cryst} = \Sigma_{hkl}|F_o(hkl) - F_c(hkl)|/\Sigma_{hkl}|F_o(hkl)|$, where F_o and F_c are observed and calculated structure.
[c] Values indicate root-mean-square deviations in bond lengths, bond angles, and B-factors of bonded atoms.
[d] Parentheses indicate statistics for the high resolution data bin for x-ray data and refinement.

3′-OH (Fig. 8*A*). A carboxylate functional group is required at positions 70 and 94, insofar as glutamate substitutions at either site restored activity *in vivo*, whereas the asparagine changes were lethal (Table II). The failure of amide functional groups at residues 70 and 94 to support activity implies that the relevant function of these aspartates is to accept a pair of hydrogen bonds from water and AdoMet, respectively. The Asp-78 side chain coordinates the AdoMet amine via a water molecule (Fig. 8*A*) and also interacts directly with the Lys-81 side chain. Replacing Asp-78 with asparagine was unconditionally lethal; a glutamate substitution restored growth at 25 and 30 °C but was lethal at 37 °C.

Tyr-124 and Ile-95 form a hydrophobic sandwich around the adenine of AdoMet. Whereas a I95A/Y124A double mutation was lethal in yeast, the I95A single mutation had no effect on growth, and the Y124A single mutations conferred a ts growth defect (21). In addition to stacking on the purine, Tyr-124 engages in a hydrogen bond from its phenolic oxygen to both the Ser-139 and Ser-142 O-γ atoms. Ser-142 C-β and O-γ atoms are in VDW contact with the ribose O-4 atom of AdoMet (Fig. 8*A*). Here we found that replacing Tyr-124 with phenylalanine rescued the ts defect of the alanine mutant and restored growth at 37 °C (Table II). We surmise that the VDW stacking interaction with the AdoMet adenine is the relevant contribution to Ecm1 function *in vivo*.

Amino acids that comprise the GTP-binding pocket include Phe-141, His-144, Tyr-145, Phe-214, Glu-225, and Tyr-284 (Fig. 8*C*). We showed previously that Phe-141, which makes multiple van der Waals contacts with the cap guanine and ribose, is essential for Ecm1 function in yeast (21). Here we tested the effects of alanine substitutions for His-144, Tyr-145, Phe-214, and Glu-225. Of these changes, only the loss of the Tyr-145 side chain resulted in unconditional lethality. Tyr-145 is situated at the interface between the methyl donor and acceptor sites. It makes extensive van der Waals contacts to the adenine base and ribose sugar of AdoMet (via the C-β, C-γ, C-δ1, and C-ϵ1 atoms of Tyr-145) and a water-mediated contact to the guanine O-6 of GTP (Fig. 8). Our findings that the Y145F mutant was viable, whereas Y145S was lethal, suggest that: (i) the van der Waals interactions with AdoMet are the decisive contribution of this side chain to Ecm1 function, and (ii) the polar contacts of the hydroxyl are not essential. Furthermore, the finding that leucine sufficed in lieu of Tyr-145 implies that the aromatic ring is not strictly essential; the γ-branched leucine side chain is partially isosteric with tyrosine and could, in principle, mimic the AdoMet contacts of Tyr-145 observed in the crystal structure.

Glu-225 makes hydrogen bonds to the guanine N-1 atom and the Tyr-212 hydroxyl and is also poised to interact with the exocyclic C-2 amine of guanine (Fig. 8*C*), suggesting that this residue contributes to cap acceptor specificity. The E225A mutation resulted in a slow growth phenotype at 25 and 30 °C and failure to grow at 37 °C (Table II). Growth was restored by conservative changes to either glutamine or aspartate. The fact that the carboxylate functional group can be replaced by an amide suggests that a neutral hydrogen bond sufficed for activity *in vivo*. Phe-214 makes van der Waals contacts to the C-2 amine, N-2, and N-3 of guanine via the tyrosine C-δ2 and C-ϵ2 atoms (Fig. 8*C*). Changing Phe-214 to alanine did not affect growth at 25 and 30 °C, but was lethal at 37 °C. The conservative leucine change restored viability at 37 °C (scored as ++), indicating that the aliphatic contacts were most relevant for growth at higher temperature. Given that the contacts of Phe-214 and Glu-225 with the edge of the guanine base partially overlap and the similarity of the ts phenotypes elicited by the F214A and E225A mutations, these two residues might be functionally redundant as determinants of guanine specificity. The Tyr-212 side chain lines the wall of the guanosine-binding pocket, and although it is not in direct contact with the guanine, it donates a hydrogen bond from its hydroxyl to the Glu-225 carboxylate. Changing Tyr-212 to alanine elicited a ts growth defect (Table II). The conservative Y212F change restored growth at 37 °C, indicating that the ts growth defect of Y212A was probably not caused by loss of its polar interaction with Glu-225.

His-144 donates a hydrogen bond from N-ϵ to guanine O-6 (Fig. 8*C*) and might thereby contribute to methyl acceptor specificity. However, we found that replacing His-144 with alanine had no effect on yeast growth at 25 or 30 °C, although this change did slow growth at 37 °C (Table II). It is conceivable that the guanine O-6 contact to His-144 and the water-mediated contact to the Tyr-145 hydroxyl are functionally redundant.

Lys-75, Arg-106, and Asn-51 are located near the triphosphate bridge of the cap methyl acceptor in the Ecm1 crystal structure (Fig. 8*C*). Arg-106 is strictly essential for Ecm1 activity *in vivo*, as gauged by the lethality of the R106A, R106K, and R106Q alleles. We showed previously that changing Lys-75 to Ala results in slow growth at 25 and 30 °C and no growth at 37 °C (21). Here we found that full activity was restored by introducing an arginine (but not a glutamine), signifying that positive charge is the relevant property of this side chain (Table II). We showed previously that changing Asn-51 to alanine had no effect on yeast growth at 25 or 30 °C, but was lethal at 37 °C. Thus, although Asn-51 comprises part of the positive groove through which the triphosphate bridge passes, its hydrogen bonding potential is not strictly critical. Nonetheless, we found presently that changing the neutral asparagine to its acidic isostere aspartate resulted in unconditional lethality (Table II). This result may attest to the importance of the positive surface potential lining the triphosphate groove of Ecm1 or to the importance of the hydrogen bonding network provided by the Asn-51 side chain between the Lys-47 carbonyl oxygen and the N-ζ of Lys-81.

Lys-81 is located on the floor of the triphosphate groove; although it does not make direct contacts with GTP or AdoMet

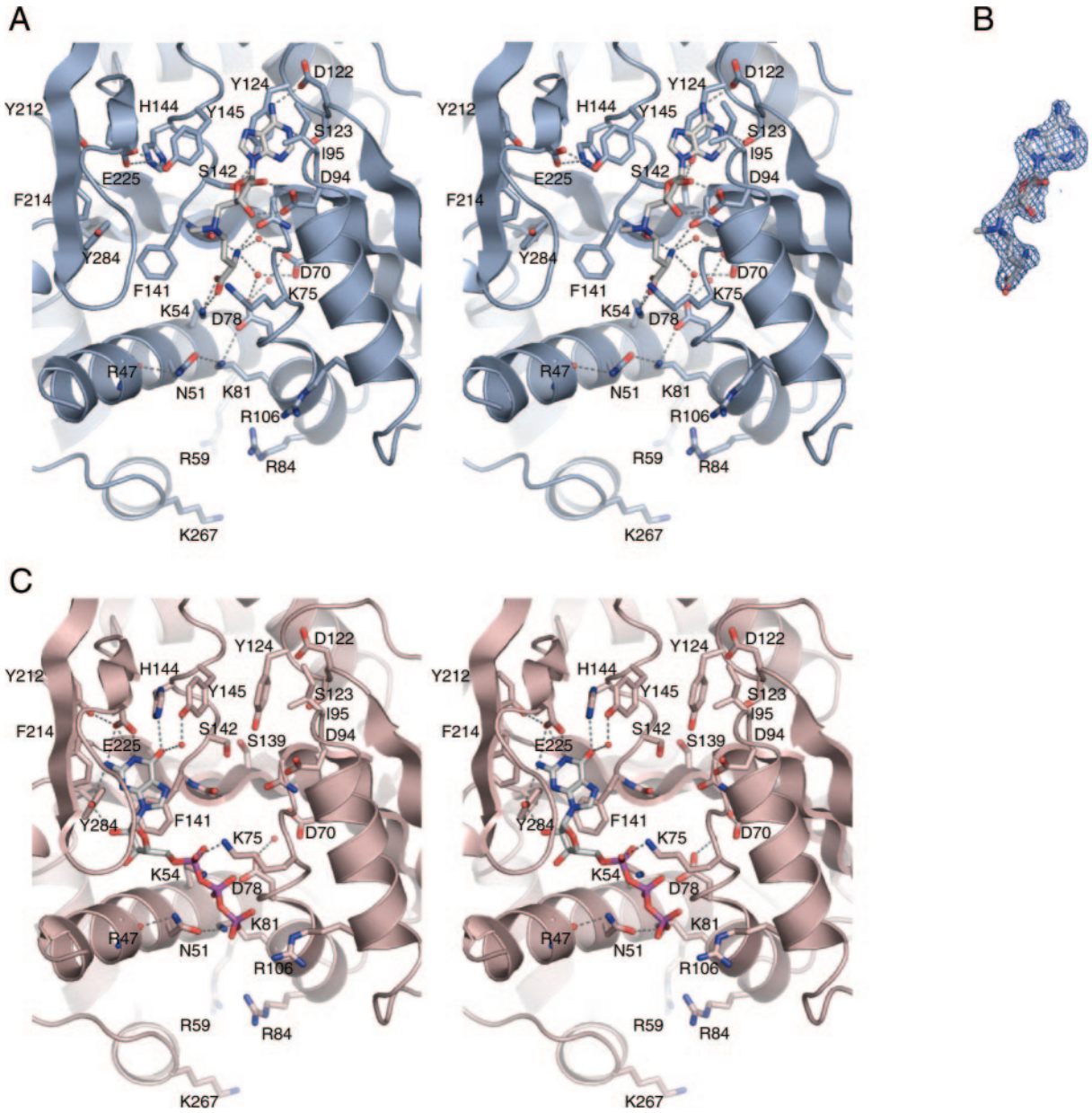

FIG. 8. **Structures of Ecm1 and the active site.** *A*, stereo view of the structure of Ecm1 in complex with aza-AdoMet. *B*, a 2.2-Å simulated annealing omit map is shown contoured at 1.0σ covering the aza-AdoMet ligand. *C*, stereo view of the Ecm1 structure (Protein Data Bank accession code 1RI2) in complex with the GTP portion of the m^7GpppG cap analog. Potential hydrogen-bonding interactions are shown by *dashed lines*; waters are rendered as *red spheres*. Amino acid residues are labeled and shown in *stick* representation. aza-AdoMet and GTP are shown in *stick* representation. The figure was generated with Pymol software (W. L. DeLano, www.pymol.org).

in the crystal structures, Lys-81 does contact Asn-51 and Asp-78 (an essential side chain). Lys-81 is essential for Ecm1 function *in vivo*; the alanine mutation was lethal as were the conservative arginine and glutamine mutations (Table II).

The structure of GTP-bound Ecm1 highlighted a candidate surface docking site for the 5′-RNA polynucleotide along a track extending away from the triphosphate bridge (21). Here we mutated three of the positively charged surface residues that lie along this track (Arg-59, Arg-84, and Lys-267) but found that no single alanine mutation had an effect on *abd1*Δ complementation (Table II).

Effects of Selected Mutations on Methyltransferase Activity in Vitro—The effects of five alanine mutations that were lethal *in vivo* on cap methyltransferase activity *in vitro* were assessed by producing the K54A, D70A, D78A, D94A, and F141A proteins in *E. coli* and purifying them from a soluble extract by nickel-agarose chromatography in parallel with wild-type Ecm1 (Fig. 9*A*). Aliquots (2 μg) of each protein were assayed for methyl transfer from 50 μM [^{3}H-CH$_3$]AdoMet to 5 mM GTP (Fig. 9*B*). All of the mutations suppressed methyltransferase activity to ≤3% of the wild-type level. Thus, *in vivo* lethality correlated with loss of catalytic activity for this set of mutations. The essentiality of Lys-54, Asp-70, Asp-78, and Asp-94 is consistent with the direct or water-mediated contacts made by these side chains to the AdoMet carboxyl, amine, and ribose moieties. The loss of function caused by the elimination of Phe-141 attests to the importance of its van der Waals interactions with the guanosine methyl acceptor seen in the Ecm1-GTP cocrystal.

DISCUSSION

Insights to Methyl Acceptor Specificity—Here we showed that Ecm1 methylates GpppA, GTP, and dGTP but not ATP, ITP, XTP, CTP, or UTP. The guanine specificity of the cap methylation reaction is consonant with the network of con-

TABLE II
Mutational effects on Ecm1 activity in yeast

Ecm1 complementation of an *abd1Δ* yeast mutant was tested by plasmid shuffle as described under "Experimental Procedures."

Ecm1 allele	*abd1Δ* complementation			Atomic contacts/proximity
	25°C	*30°C*	*37°C*	
N51A[a]	+++	+++	−	Lys-81, cap triphosphate
N51D	−	−	−	
K54A[a]	−	−	−	AdoMet carboxyl
K54R	−	−	−	
K54Q	−	−	−	
R59A	+++	+++	+++	
D70A	−	−	−	AdoMet amine (via HOH)
D70N	−	−	−	
D70E	+++	+++	+++	
K75A[a]	++	++	−	Cap triphosphate
K75R	+++	+++	+++	
K75Q	++	+	+	
D78A	−	−	−	Lys-81, AdoMet amine (via HOH)
D78N	−	−	−	
D78E	+++	+++	−	
K81A[a]	−	−	−	Asp-78, Asn-51
K81R	−	−	−	
K81Q	−	−	−	
R84A	+++	+++	+++	
D94A[a]	−	−	−	AdoMet ribose hydroxyls
D94N	−	−	−	
D94E	+++	+++	+++	
R106A	−	−	−	Cap triphosphate
R106K	−	−	−	
R106Q	−	−	−	
Y124A[a]	+++	+++	−	AdoMet adenine, Ser-142
Y124F	+++	+++	+++	
H144A	+++	+++	++	Cap guanine
Y145A	−	−	−	AdoMet, cap guanine (via HOH)
Y145F	+++	+++	+++	
Y145L	+++	+++	+++	
Y145S	−	−	−	
Y212A	+++	+++	−	Glu-225
Y212F	+++	+++	+++	
F214A	+++	+++	−	Cap guanine
F214L	+++	+++	++	
E225A	++	++	−	Cap guanine
E225Q	+++	+++	+++	
E225D	+++	+++	+++	
K267A	+++	+++	+++	

[a] Ecm1 alleles reported previously (21).

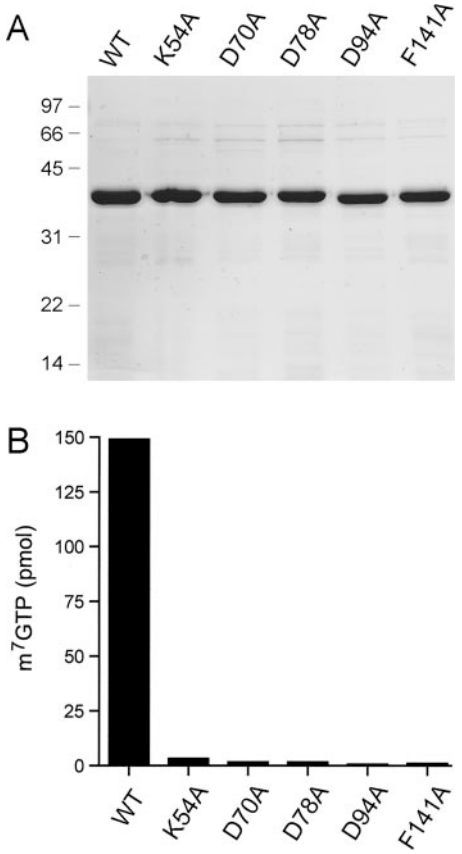

FIG. 9. **Effects of alanine mutations on methyltransferase activity in vitro.** *A*, aliquots (5-μg) of the nickel-agarose fractions of wild-type (*WT*) Ecm1 and mutants K54A, D70A, D78A, D94A, and F141A were analyzed by SDS-PAGE. Polypeptides were visualized by staining the gel with Coomassie Blue dye. The positions and sizes (in kDa) of marker proteins are indicated on the *left*. *B*, reaction mixtures (20-μl) containing 50 mM Tris-HCl (pH 7.5), 5 mM DTT, 5 mM GTP, 50 μM [^{3}H-CH$_3$]AdoMet and 2 μg of either WT or mutant Ecm1 proteins were incubated for 60 min at 37 °C. Aliquots of the mixtures (5-μl) were spotted on polyethyleneimine cellulose TLC plates, which were developed with 0.2 M $(NH_4)_2SO_4$. The extent of [^{3}H-CH$_3$]m^{7}GTP formation is plotted for each enzyme.

tacts seen in the Ecm1-cap cocrystal (21), which entail hydrogen bonding interactions between conserved protein side chains and the guanine N-1, N-3, and O-6 atoms and also van der Waals and polar contacts with the guanine exocyclic 2-NH_2. In the Ecm1-cap structure, the Glu-225 carboxylate is poised to make a bidentate hydrogen bond to the protonated N-1 and the exocyclic 2-NH_2. Because the N-1 atom of adenosine is unprotonated, an interaction of Glu-225 with adenine would likely be disallowed. Contacts of His-144 and Tyr-145 to the purine O-6 atom provide additional discrimination between guanine and adenine. The guanine exocyclic 2-NH_2 in the Ecm1-cap cocrystal projects into a pocket where it makes van der Waals contacts with Pro-175, Phe-214, and Tyr-284 and polar contacts with Glu-225 and the Tyr-284 hydroxyl group. The fact that ITP and XTP are not substrates for Ecm1 indicates that these contacts to the exocyclic 2-NH_2 are important for substrate binding.

The results of the present mutational analysis of Ecm1 indicate that few of the individual side chain contacts to the edge of the guanine base are essential *per se* for Ecm1 function *in vivo*. We infer that there is functional redundancy, which can ultimately be gauged by analyzing the combinatorial effects of conservative mutations in residues that comprise the guanine-binding pocket. Phe-141, which is located on the floor of the guanine-binding pocket, is essential for cap methyltransferase activity *in vivo* and *in vitro*. We infer that the van der Waals interactions of Phe-141 with the cap guanine and ribose are critical for substrate binding, although not necessarily for guanosine specificity.

The role of the cap guanine nucleoside sugar was surmised from the effects of 2′- and 3′-sugar modifications on methyltransferase activity. dGTP was slightly more effective as an acceptor than GTP, implying that the 2′-OH is noncontributory to substrate specificity. The Ecm1-cap cocrystal highlighted a hydrogen bond between the ribose 2′-OH and the phenolic oxygen of Tyr-284; the latter also donates hydrogen bonds to the N-3 and exocyclic 2-NH_2 of the cap guanine. We surmise that the sugar contact of Tyr-284 is not important for Ecm1 function *in vitro*. The addition of a 3′-OMe group to the guanosine sugar reduced methyltransferase activity by a factor of 3. The Ecm1-cap cocrystal showed that the ribose 3′-OH engages in a hydrogen bond with Asn-50. The fact that Ecm1 retains activity with 3′-OMe-GTP and ddGTP suggests that this hydrogen bond is not essential. ddGTP was methylated 25% as well as GTP and 20% as well as dGTP. The pairwise comparison of ddGTP to dGTP implies that the 3′-OH group contributes a 5-fold enhancement of methyltransferase activity.

Finally, the contributions of the cap-distal phosphate of the cap triphosphate bridge are inferred from a comparison of the Ecm1 activity with GTP, GpppA, and GDP substrates. Removal

of the distal phosphate reduced activity by a factor of 3. This effect could be caused either by a loss of protein contacts to the missing γ phosphate or the introduction an additional negative charge on the β phosphate in lieu of the neutral β–γ bridging oxygen of GTP. The presence of a cap-proximal nucleoside in the cap analog GpppA enhanced activity by increasing the affinity of Ecm1 for the cap acceptor. This result implies that either: (i) Ecm1 makes contacts with the cap-proximal nucleoside that contribute to substrate affinity or (ii) neutralization of the second negative charge on the GTP γ phosphate by the nucleoside 5′-phosphoester enhances substrate affinity. In either event, it seems likely that Ecm1 will enjoy even higher affinity for a capped RNA polynucleotide than it does for a cap dinucleotide, thereby ensuring that methylation will be directed to nascent pre-mRNA rather than free GTP. (Preliminary studies show that Ecm1 can bind *in vitro* to the phosphorylated carboxyl-terminal domain of RNA polymerase II; such an interaction could target cap methylation to nascent pre-mRNAs *in vivo*.)

Product and Substrate Analogs as Inhibitors of Cap Methylation—Cap methylation has been invoked as a target for antiinfective drug discovery. This idea is supported by the efficacy of AdoHcy hydrolase inhibitors against poxviruses and many RNA viruses that encode their own cap methylating enzymes (33). Inhibition of cellular AdoHcy hydrolase elevates intracellular levels of AdoHcy by preventing its cleavage to homocysteine and adenosine. Here we showed that Ecm1 is inhibited by the product AdoHcy, a finding that agrees with prior reports that viral, fungal, and human guanine N-7 methyltransferases are also sensitive to product inhibition (3, 10, 12, 16). Blocking cellular AdoHcy hydrolase is an indirect and relatively nonspecific strategy to inhibit capping. Direct targeting of the cap methylating enzyme offers a potentially superior approach with fewer off-target effects. An ideal inhibitor might be a bifunctional molecule that simultaneously occupies the methyl donor and methyl acceptor sites on the enzyme. As a preliminary test of affinity for the methyl donor site, we tested inhibition of Ecm1 by several analogs of AdoMet, including sinefungin, aza-AdoMet, and carbocyclic aza-AdoMet. We operationally define weak inhibitors as those that are obviously less potent than the product AdoHcy and a good inhibitor as one that is more potent than AdoHcy. By this criterion, the aza-AdoMet derivatives are weak inhibitors of Ecm1. The crystal structure of the Ecm1·aza-AdoMet complex reveals virtually no difference compared with the Ecm1-AdoMet structure. This is in contrast to the case of the *E. coli* MetJ repressor, whereby MetJ/AdoMet and MetJ/aza-AdoMet crystal structures reveal major differences in the conformation and protein contacts of the methionine components of AdoMet *versus* aza-AdoMet ligands (34). However, given that Ecm1 makes no direct contacts to the AdoMet methyl carbon or the AdoMet sulfur (the latter atom being substituted by nitrogen in the aza compound), it is not surprising that the Ecm1/AdoMet and Ecm1/aza-AdoMet structures are so similar.

How then should we account for the lower binding affinity to aza-AdoMet? The pK_a of the tertiary amine of aza-AdoMet is reported to be 7.1 (31, 34), in which case the nitrogen center would be predominantly uncharged under the conditions used here to assay Ecm1 activity, but predominantly charged under the conditions used to grow the crystals. However, it is unlikely that the relatively low inhibitory potency of aza-AdoMet is caused only by the absence of a positive charge equivalent to the AdoMet sulfonium group, because the neutral AdoHcy product is itself an effective competitor for the methyl donor site. Perhaps the weaker affinity of aza-AdoMet is caused by subtle differences in bond geometry and electrostatics around the nitrogen center. It is noteworthy that Reich and Mashoon (35) found aza-AdoMet to be 5-fold less potent than AdoHcy as an inhibitor of the EcoRI DNA methylase. Based on the findings here, we would not regard aza-AdoMet as a promising scaffold on which to build a bisubstrate inhibitor of cap methylation. Nonetheless, the fact that the carbocyclic derivative of aza-AdoMet was 3-fold more potent than the ribose compound indicates that the ribose 4 oxygen is dispensable. In the Ecm1 structure, the ribose O-4 of aza-AdoMet makes a VDW contact to Ser-142 C-β (Fig. 8*A*).

Sinefungin has been reported to be a very potent inhibitor of vaccinia virus cap guanine N-7 methyltransferase (K_i = 12 nM sinefungin) and an inhibitor of vaccinia replication in cell culture (30). Sinefungin is 100-fold more potent than AdoHcy (K_i = 1.3 μM) as an inhibitor of the vaccinia methyltransferase. We find here that sinefungin is only 2–3-fold more potent than AdoHcy as an inhibitor of a cellular cap methyltransferase Ecm1. If sinefungin exerts similar effects on mammalian cap methyltransferase, it would suggest that the anti-poxviral effects of noncytotoxic doses of sinefungin correlate with selectivity for the viral *versus* host capping systems. Further studies of the antiviral mechanism of sinefungin are underway. In the meantime, we regard sinefungin as a useful scaffold upon which to design a bisubstrate inhibitor of cap methylation.

Acknowledgments—We thank Minmin Yang (Auburn University) for generously providing aza-AdoMet and carbocyclic aza-AdoMet for use in this study.

REFERENCES

1. Shuman, S. (2002) *Nat. Rev. Mol. Cell. Biol.* **3,** 619–625
2. Shuman, S. (2001) *Cold Spring Harbor Symp. Quant. Biol.* **66**, 301–312
3. Martin, S. A., and Moss, B. (1975) *J. Biol. Chem.* **250,** 9330–9335
4. Martin, S. A., and Moss, B. (1976) *J. Biol. Chem.* **251,** 7313–7321
5. Cong, P., and Shuman, S. (1992) *J. Biol. Chem.* **267,** 16424–16429
6. Higman, M. A., Bourgeois, N., and Niles, E. G. (1992) *J. Biol. Chem.* **267,** 16430–16437
7. Higman, M. A., Christen, L. A., and Niles, E. G. (1994) *J. Biol. Chem.* **269,** 14974–14981
8. Higman, M. A., and Niles, E. G. (1994) *J. Biol. Chem.* **269,** 14982–14987
9. Mao, X., and Shuman, S. (1994) *J. Biol. Chem.* **269,** 24472–24479
10. Mao, X., and Shuman, S. (1996) *Biochemistry* **35,** 6900–6910
11. Niles, E. G., Christen, L., and Higman, M. A. (1994) *Biochemistry* **33,** 9898–9903
12. Mao, X., Schwer, B., and Shuman, S. (1995) *Mol. Cell. Biol.* **15,** 4167–4174
13. Mao, X., Schwer, B., and Shuman, S. (1996) *Mol. Cell. Biol.* **16,** 475–480
14. Wang, S. P., and Shuman, S. (1997) *J. Biol. Chem.* **272,** 14683–14689
15. Schwer, B., Saha, N., Mao, X., Chen, H. W., Shuman, S. (2000) *Genetics* **155,** 1561–1576
16. Saha, N., Schwer, B., and Shuman, S. (1999) *J. Biol. Chem.* **274,** 16553–16562
17. Pillutla, R. C., Yue, Z., Maldonado, E., and Shatkin, A. J. (1998) *J. Biol. Chem.* **273,** 21443–21446
18. Tsukamoto, T., Shibagaki, Y., Niikura, Y., and Mizumoto, K. (1998) *Biochem. Biophys. Res. Commun.* **251,** 27–34
19. Yamada-Okabe, T., Mio. T., Kashima, Y., Matsui, M., Arisawa, M., and Yamada-Okabe, H. (1999) *Microbiology* **145,** 3023–3033
20. Hausmann, S., Vivares, C. P., Shuman, S. (2002) *J. Biol. Chem.* **277,** 96–103
21. Fabrega, C., Hausmann, S., Shen, V., Shuman, S., and Lima, C. D. (2004) *Mol. Cell* **13,** 77–89
22. Takata, Y., Huhang, Y., Komoto, J., Yamada, T., Konishi, K., Ogawa, H., Gomi, T., Fujioka, M., and Takusagawa, F. (2003) *Biochemistry* **42,** 8394–8402
23. Yang, M., Ye, M., and Schneller, S. W. (2004) *J. Org. Chem.* **69,** 3993–3996
24. Otwinowski, Z., and Minor, W. (1997) *Methods Enzymol.* **276,** 307–326
25. Collaborative Computational Project (1994) *Acta Crystallogr. Sect. D* **50,** 760–763
26. Jones, T. A., Zou, J. Y., Cowan, S. W., and Kjeldgaard, M. (1991) *Acta Crystallogr. Sect. A* **47,** 110–118
27. Brunger, A. T., Adams, P. D., Clore, G. M., DeLano, W. L., Gros, P., Grosse-Kunstleve, R. W., Jiang, J. S., Kuszewski, J., Nilges, M., Pannu, N. S., Read, R. J., Rice, L. M., Simonson, T., and Warren, G. L. (1998) *Acta Crystallogr. Sect. D* **54,** 905–921
28. Barbosa, E., and Moss, B. (1978) *J. Biol. Chem.* **253,** 7692–7697
29. Ghosh, A. K., and Liu, W. (1996) *J. Org. Chem.* **61,** 6175–6182
30. Pugh, C. S., Borchardt, R. T., and Stone, H. O. (1978) *J. Biol. Chem.* **253,** 4075–4077
31. Thompson, M. J., Mekhalfia, A., Jakeman, D. L., Phillips, S. E. V., Phillips, K., Porter, J., and Blackburn, G. M. (1996) *Chem. Commun.* (*Camb.*) 791–792
32. Minnick, A. A., and Kenyon, G. L. (1988) *J. Org. Chem.* **53,** 4952–4961
33. Liu, S., Wolfe, M. S., and Borchardt, R. T. (1992) *Antiviral Res.* **19,** 247–265
34. Thompson, M. J., Mekhalfia, A., Hornby, D. P., and Blackburn, G. M. (1999) *J. Org. Chem.* **64,** 7467–7473
35. Reich, N. O., and Mashoon, N. (1990) *J. Biol. Chem.* **265,** 8966–8970